



# Exploring climate shifts in the Ganga–Brahmaputra basin based on rainfall and temperature variability

Kavita Kaushik · Arvind Chandra Pandey ·  
Chandra Shekhar Dwivedi

Received: 9 March 2024 / Accepted: 19 August 2024 / Published online: 27 August 2024  
© The Author(s), under exclusive licence to Springer Nature Switzerland AG 2024

**Abstract** Climate change has a significant impact on the Ganga–Brahmaputra (GB) basin, the major food belt of India, which frequently experiences flooding and varied incidences of drought. The current study examines the changing trend of rainfall and temperature in the GB basin over a period of 30 years to identify areas at risk with an emphasis on the Paris Agreement’s mandate to keep increasing temperatures below 2 °C. The maximum temperature anomaly in the middle Ganga plains recorded an increase of more than 1.5 °C year<sup>-1</sup> in 1999, 2005, and 2009. Some extreme events were observed in the Brahmaputra basin during 1999, 2009, and 2010, where a prominent temperature increase of 1.5 °C year<sup>-1</sup> was observed. The minimum temperature revealed an increasing trend for the G-B basin with an anomalous increase of 0.04 to 0.06 °C year<sup>-1</sup>. The rainfall variability across the Ganga basin shows a rising tendency over the lower Ganga region while the Brahmaputra basin showed a downward trend. To identify the statistical relation between the Global climatic

oscillations and regional climate, Standardized Precipitation Index (SPI) and Niño 3.4 were used. The wet and dry period estimation shows a rise in flood conditions in the Ganga basin whereas, in the Brahmaputra basin, an increase in drought frequency was observed. The correlation based on Niño 3.4 and SPI3 presents a negative relation for the monsoon season in the G-B basin revealing a situation of drought occurrence (SPI3 below 0) with increased Niño 3.4 values (El Niño above +0.4C).

**Keywords** Climate change · Ganga–Brahmaputra basin · Standardized Precipitation Index (SPI) · Global oscillations · Temperature and rainfall variability

## Introduction

The Ganga Brahmaputra basin is rich in water resources; however, the changing climate leading to uncertainty in water availability has challenged the region in ensuring basic necessities of the population (Rasul, 2015). The majority of the basin’s population (80% out of 625 million) depends on the agriculture sector and utilizes the river water for their day-to-day life (Pandey et al., 2022). The Ganga–Brahmaputra flow is highly seasonal and is heavily affected by the monsoon rainfall (Chowdhury & Ward, 2004). The monsoon rainfall has a significant impact on the people, economy, agriculture, and environment of the

---

K. Kaushik · A. C. Pandey (✉) · C. S. Dwivedi  
Department of Geoinformatics, School of Natural  
Resource Management, Central University of Jharkhand,  
Ranchi 835222, India  
e-mail: arvindchandrap@yahoo.com

K. Kaushik  
e-mail: kaushikkavita99@gmail.com

C. S. Dwivedi  
e-mail: chandra.dwivedi@cuja.ac.in

area. Due to climate change, the increased ability of the warmer atmosphere to hold water has resulted in increased rainfall (Uhe et al., 2019) and its related disasters. Being the major food belt of the country, any negative impact of climate change on the basin would affect a large sum of the population.

Water quality will be impacted by socioeconomic change because water diversion tactics, population growth, and industrial development disrupt the water balance and increase nutrient fluxes from agricultural, urban areas, and atmospheric deposition (Whitehead et al., 2018). Climate alters the flood flows and changes the pollution dilution factors in the rivers, including other processes controlling the quality of water. It also affects the basin discharge characteristics leading to more severe and frequent flooding (Immerzeel, 2008), as it intensifies the hydrological cycle which leads to increased precipitation with higher frequency, intensity, and the severity of floods (Apurv et al., 2015). The upper part of the Ganga–Brahmaputra catchment comprises lofty snow mountains that contributes highly towards the river discharge of the rivers due to snowmelt (Barman & Bhattacharjya, 2015). Under the recent climatic conditions, the snow cover area changes are expected to bear effects on the hydrological cycle (Parajuli et al., 2021). The climate change in the Brahmaputra basin is also a major concern for Bangladesh because of its influence on the floods and hydrological droughts.

Floods and droughts account for a major share of natural disasters caused by the extreme meteorological occurrences (Parajuli et al., 2021). The increasing trend in temperature and its impact on local climate has altered the drought events frequency and severity with respect to which the changing climate drought analysis studies have gained more attention. To assess climate-induced changes in any region, rainfall and temperature data of at least thirty years is vital to suggest adaptation strategies (Yvonne et al., 2020). To define trend, the general movement of the series is observed over an extended period of time (Panda & Sahu, 2019). Numerous techniques, including parametric techniques like the *T*-test, *F*-test, and liner regression as well as nonparametric techniques like the Mann–Kendall test, the Krushal-Wallis test, and Sen's slope estimators, have been used in prior research to assess climate variability and its trends. To analyze patterns in time series, different techniques are used such as autoregressive (AR), moving

average (MA), exponential smoothing (ES), and integrated ARMA (ARIMA) (Roshani et al., 2023), neural network, seasonal decomposition, and spectral analysis (Mahmood et al., 2019).

Ganga–Brahmaputra basin has shown an insignificant downward trend during 1960 to 2010 estimated through Mann–Kendall trend analysis and annual discharge variation lines. The rivers showed the trend of “wet-dry” during the time period of 1960–1990 wet and 1990–2010 dry (Shi et al., 2019). Standardized Precipitation Index has been widely used to compare accumulated precipitation over different time scales with the historical precipitation to quantify the wet and dry areas. Using a time series of cumulative precipitation with a probability-based indicator, the SPI index calculates the degree of deviation of a certain time from the average of the series (Guhathakurta et al., 2017). The potential of SPI has also been explored for monitoring flood risk (Seiler et al., 2002) and droughts. The different time scales can provide insight on different types of droughts (meteorological, agricultural, or hydrological). The SPI has a profound performance while presenting precipitation anomaly as compared to other drought indices (McKee et al., 1993) and it requires precipitation data only as input and hence is suitable for monitoring flood and drought conditions.

Various studies have used SPI and SPEI for trend analysis, identification of drought, and for the estimation of wet and dry periods over the past years for climate change analysis (Komuscu, 1999; Mishra & Desai, 2005; Niranjana Kumar et al., 2013; Alam et al., 2017; Bhunia et al., 2020; Das et al., 2020). Over the Indian region, drought characteristics have been analyzed using various indices, including SPI, SPEI, HMM-DI, and GMM-DI (Mondal & Lakshmi, 2021) over the time period of 103 years (1901–2004) (Mallya et al., 2016) revealing drought prone condition in the upper middle Gangetic plains with an occurrence frequency of 40–45% (Nath et al., 2017; Singh & Shukla, 2020). The tropical sea surface anomalies significantly affect the variability of droughts in India (Guhathakurta et al., 2017). The ENSO influence on drought phenomena has been evaluated on a large scale (Pervez & Henebry, 2015; Trenberth & Hoar, 1997) where correlation and wavelet transform analyses revealed a significant negative correlation between SPI12 and Niño 3.4, and Niño 4 (Loaiza Cerón et al., 2020). The global climatic

oscillations (DMI, TNI, Niño 3.4, Niño 4) can be used to access their impact over the regional climate.

The climate variability and trend knowledge are important for accurate forecasting of climate variables, management, mitigating flood and drought situations, and adaptation measures to cope with climate change. The Paris Agreement’s goal is to pursue efforts to keep temperature increases to 1.5 °C and keep global warming below 2 °C at industrial levels (UNFCCC, 2015) has triggered the need to identify the regions with increasing temperature.

**Study area**

The Ganga–Brahmaputra basin together constitutes an extensive area of approximately 1,800,000 km<sup>2</sup> (Fig. 1). The Ganga river drains almost one-fourth of India’s territory and supports millions of people in the country. It rises in the southern Himalayas travels through the plains and empties into the Bay of Bengal (Ahmed, 2022). Alaknanda, Bhagirathi, Mandakini, Dhauliganga, and the Pindar are the five headstreams of the river. The Ganga river basin encompasses an area of 1,086,000 km<sup>2</sup>. The annual average rainfall varies widely in the basin with approximately 760 mm on the western part of the basin to more than 2200 mm on the eastern side (Ahmed, 2022; Gain & Giupponi, 2014).

The Brahmaputra is a transboundary river, it originates in China flows for 1130 km to the north-eastern part of India and flows for a distance of 1130 kms, and then enters Bangladesh then emptying into the Bay of Bengal (Mohammed et al., 2017; Whitehead et al., 2018). Meghna basin has been considered a part of Brahmaputra basin in this study.

**Materials and methods**

**Data used**

The present study primarily used Terra Climate data of 30 years (1991–2020) for the climate change analysis in the Ganga–Brahmaputra basin. The Terra Climate monthly minimum temperature (November–February), maximum temperature (March–June), and Precipitation data (July–October) were used to observe the changing pattern during peak season of respective parameters under study using linear trend analysis and anomaly estimation over the past years. The Hovmoller plots were based on the same dataset for different latitude, longitude, and altitude. For the altitude-based change analysis, SRTM DEM was used after resampling. SPI was calculated for the estimation of wet and dry period using the same precipitation product. Niño 3.4 data was used for analyzing the statistical relation between Niño 3.4 and SPI,

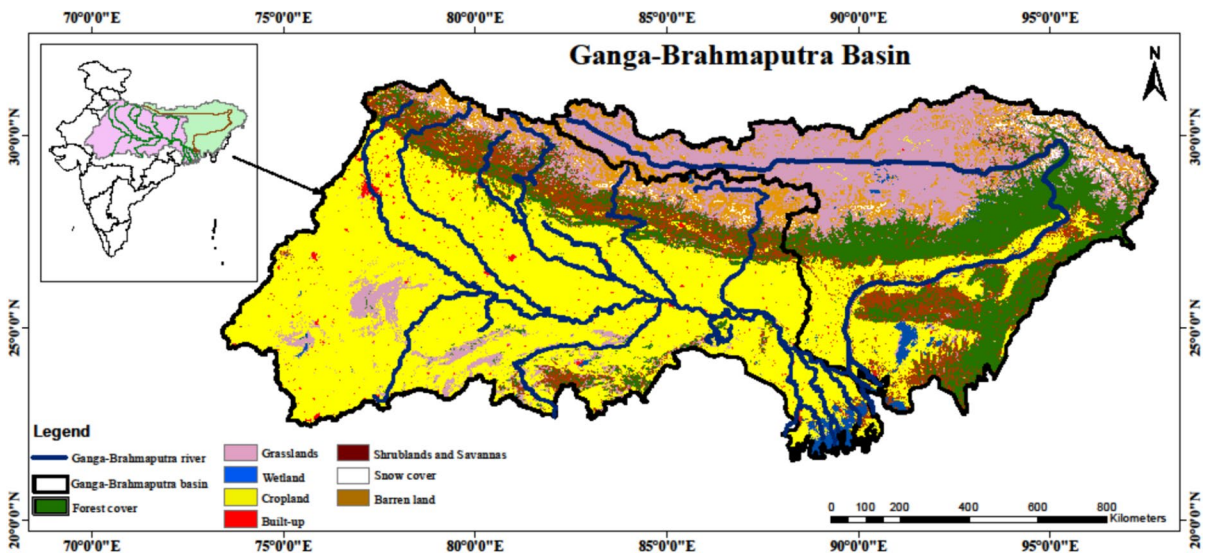


**Fig. 1** MODIS Land Use Land Cover (LULC) map of the study area

to understand the association between global and regional climatic oscillations. The dataset and methodology chart used for the present study are given in Table 1 and Fig. 2, respectively.

*Terra climate*

TerraClimate comprises of monthly climate dataset from 1958 to 2020 for global terrestrial surfaces and is updated annually with a spatial resolution of 4 km. Conceptually, anomalies from CRU Ts 4.0 and JRA55 are interpolated with WorldClim having a high spatial resolution to create a high-spatial as well as temporal resolution dataset. The created product exhibited strong validation with the

station-based observations from the Global Historical Climate Network, RAW, and SNOTEL (Abatzoglou et al., 2018).

*SRTM DEM* In order to acquire radar data for the creation of global elevation data, the shuttle Radar Topography Mission was flown from February 11 to February 22, 2000, under the international project of NASA and NGA (Fhong, 2021). The SRTM DEM was acquired using the single-pass interferometry, in which two different radar antennas are used to acquire two signals at the same time. The difference between the two signals helped in calculating the surface elevation (EROS Center, 2017).

**Table 1** Data used and their specifications

| Data used     | Resolution   | Purpose                         | Source   |
|---------------|--|---------------------------------|--|
| Terra Climate | 4 km   | Climate change analysis and SPI | Climatology lab<br><a href="https://www.climatologylab.org/terraclimate.html">https://www.climatologylab.org/terraclimate.html</a> |
| SRTM DEM      | 30 m   | Altitude characteristics        | Earthdata<br><a href="https://search.earthdata.nasa.gov/">https://search.earthdata.nasa.gov/</a>                                   |
| Niño 3.4      | 5° N to 5° S and 170° W to 120° W, monthly (1° × 1°) | correlation, Cross-correlation  | PSL NOAA<br><a href="https://psl.noaa.gov/">https://psl.noaa.gov/</a>  |

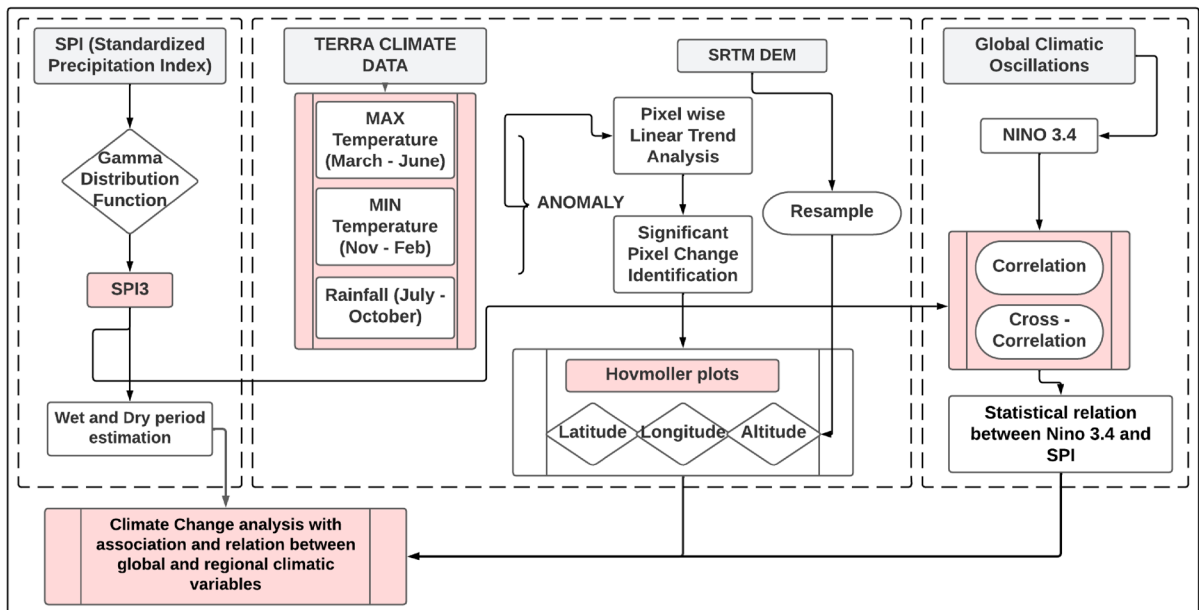


**Fig. 2** Methodology adopted for climate change analysis with association and relation between global and regional climatic variables

### Niño3.4

The average equatorial sea surface temperatures (SSTs) in the Pacific Ocean are represented by the Niño 3.4 anomaly index (5N-5S, 170W-120W). El Niño and La Niña episodes are identified by the index using a 5-month running mean. El Niño and La Niña occurrences, respectively, are characterized as the Niño 3.4 index value reaching +0.4C or -0.4C for a period of 6 months or more (NCAR, 2023).

### Methodology

For understanding the climate variability linear trend analysis was performed over the Ganga–Brahmaputra basin based on the 30 years data. The anomaly was calculated to identify the deviation of a specific climate variable, such as maximum temperature, minimum temperature, and rainfall, from its long-term average or baseline value for a particular time period and location. The obtained output was used for Hovmoller plot generation to depict the change with reference to latitude, longitude, and Altitude. To identify the areas at risk the pixels with 90% significance level in increase or decrease of any parameter were highlighted. The extreme events were identified in terms of anomalous increase or decrease over the years based on Hovmoller diagram. Standardized Precipitation Index was used to identify the wet and dry periods over the past 30 years in the GB basin and to identify the relation of regional and global oscillations based on SPI and Niño 3.4.

### Anomaly and linear trend analysis

Terra Climate data was used for the climate variability study over the Ganga–Brahmaputra basin for the last 30 years. The maximum, minimum temperature data, and rainfall data for the monsoon period were used to generate the anomaly maps and the Hovmoller plots. For the pixel-wise linear trend analysis, the Slope and Intercept were identified for the best average fit. The anomaly was calculated with the mean and standard deviation of the series to present the changing climate for the Ganga–Brahmaputra basin separately and the pixels with a significant change over the past 30 years were highlighted.

$$A = \frac{Xi - \bar{x}}{\delta}$$

where  $Xi$  is the individual observation,  $\bar{x}$  is the mean of the series (1991–2020) and  $\delta$  represents the standard deviation (Bar et al., 2021).

### Standardized Precipitation Index

Weather-related drought has been extensively described using the Standardized Precipitation Index (SPI) throughout a wide range of periods. As the index is effectively used for the analysis of dry periods, it can also be used for the analysis of wet periods across the time series data (WMO et al., 2012). Long-term precipitation data is used to generate SPI, which is then fitted to a probability density function and turned into a normal distribution with zero as the series' mean (Edwards & Mckee, 1997; Irawan et al., 2023). Positive SPI numbers imply precipitation over the median, while negative values denote precipitation below the median (Tsakiris et al., 2007). Here for the estimation of dry and wet periods, values equal or greater than 1 are referred as wet periods, and value equal or below -1 indicate drought conditions/dry periods.

The probability density function is defined as follows:

$$g(x) = \frac{1}{\beta\alpha\tau(\alpha)} x^{\alpha-1} e^{-x/\beta} \text{ for } x > 0,$$

where  $\alpha > 0$  is a shape parameter,  $\beta > 0$  is a scale parameter (1, 3, 6, 12, 48), and  $x > 0$  is the amount of precipitation (Guhathakurta et al., 2017).

### Correlation and cross-correlation

Correlation tests are statistical procedures that are commonly used in many applications. The Pearson's correlation is the most common correlation method. Cross-correlation (Salas, 1993) estimates the similarities between two variables as a function of lag. Based on the lag, the autocorrelation function correlates the variable with the previously occurring variable in the time series (Mohammadrezaei et al., 2020).

$$p = (R(0)) = \frac{\sum t((x_t - \bar{x}) \times (y_t - \bar{y}))}{\sigma(x) \times \sigma(y)}$$

where  $\bar{x}$  and  $\bar{y}$  denotes the mean of  $X$  and  $Y$ , and  $\sigma(x)$  and  $\sigma(y)$  are the standard deviations (Surmaini et al., 2015).

$$r_k = \frac{\sum_{t=1}^{N-k} (x_t - \bar{x})(x_{t+k} - \bar{x})}{\sum_{t=1}^N (x_t - \bar{x})^2}$$

where  $r_k$  is the cross-correlation of lag  $k$ , which ranges from  $-1$  to  $+1$ ,  $\bar{x}$  is the average and  $N$  is the total number of observations (Mohammadrezaei et al., 2020).

## Results

Temperature variability over the Ganga–Brahmaputra basin

*Maximum temperature over the Ganga–Brahmaputra basin*

The variability of maximum temperature over the past 30 years was studied across the Ganga–Brahmaputra

basin separately and shown in Figs. 3 and 4. The maximum temperature anomaly was calculated using the temperature data from the months of March to June (Pre-monsoon). It highlighted that over the past years major increase in temperature was observed in the northern and western parts of the Ganga basin, with a maximum of  $0.05 \text{ }^\circ\text{C year}^{-1}$  in parts of Rajasthan. The temperature increase in the Northwest and Southwest regions of Ganga basin is found to be increasing on an alarming rate with an anomaly increase of more than  $0.03 \text{ }^\circ\text{C year}^{-1}$ . Whereas, the lower Ganga Plains (parts of Jharkhand and West Bengal) show decreasing temperature trends with an anomaly range of  $-0.02 \text{ }^\circ\text{C year}^{-1}$  to  $-0.04 \text{ }^\circ\text{C year}^{-1}$ . Overall, for the Ganga basin a significant increasing trend was observed represented by highlighting the pixels with a significance level of 90% over the anomaly map.

Apart from the overall analysis of the basin, Hovmoller plots were generated for a better understanding of the changing pattern considering different latitudes, longitudes, and altitude. During the years 1999, 2005, and 2009, the temperature increase from the previous years was more than  $1.5 \text{ }^\circ\text{C}$  along the

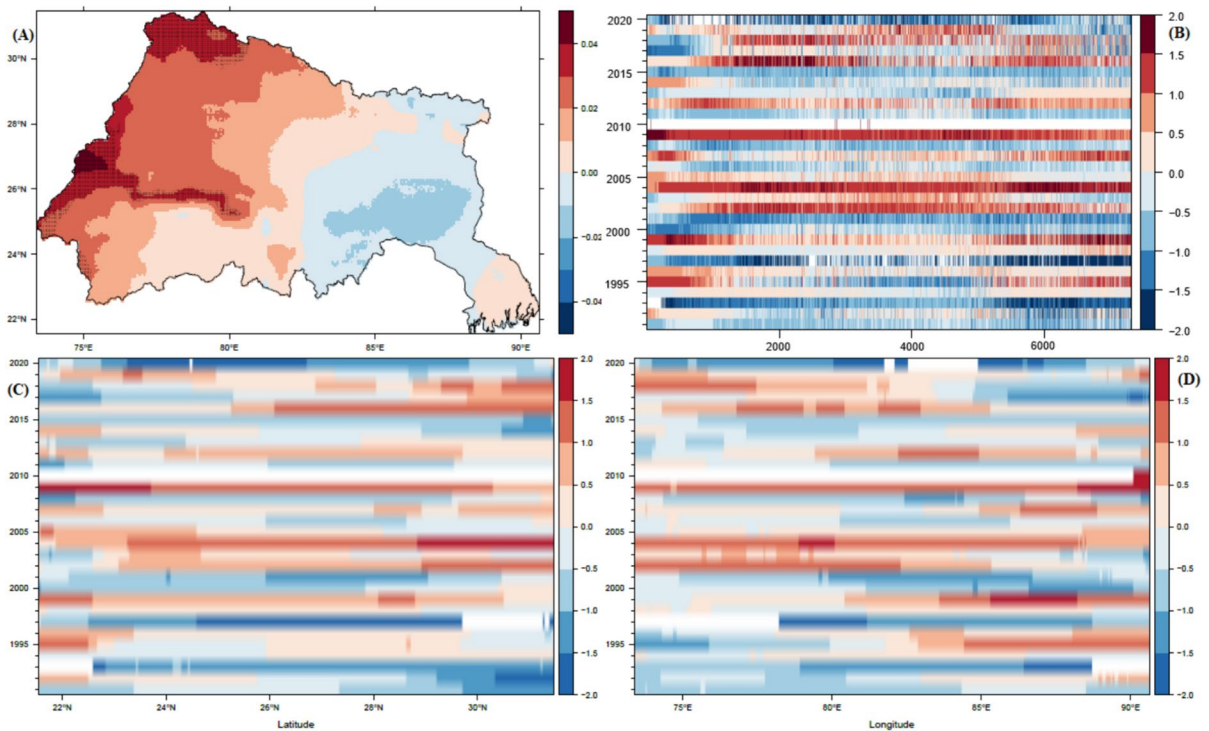


**Fig. 3** Maximum temperature variability over the Ganga basin during the summer season (anomaly map (A) and Hovmoller diagram for altitude (B), latitude (C), and longitude (D), respectively)

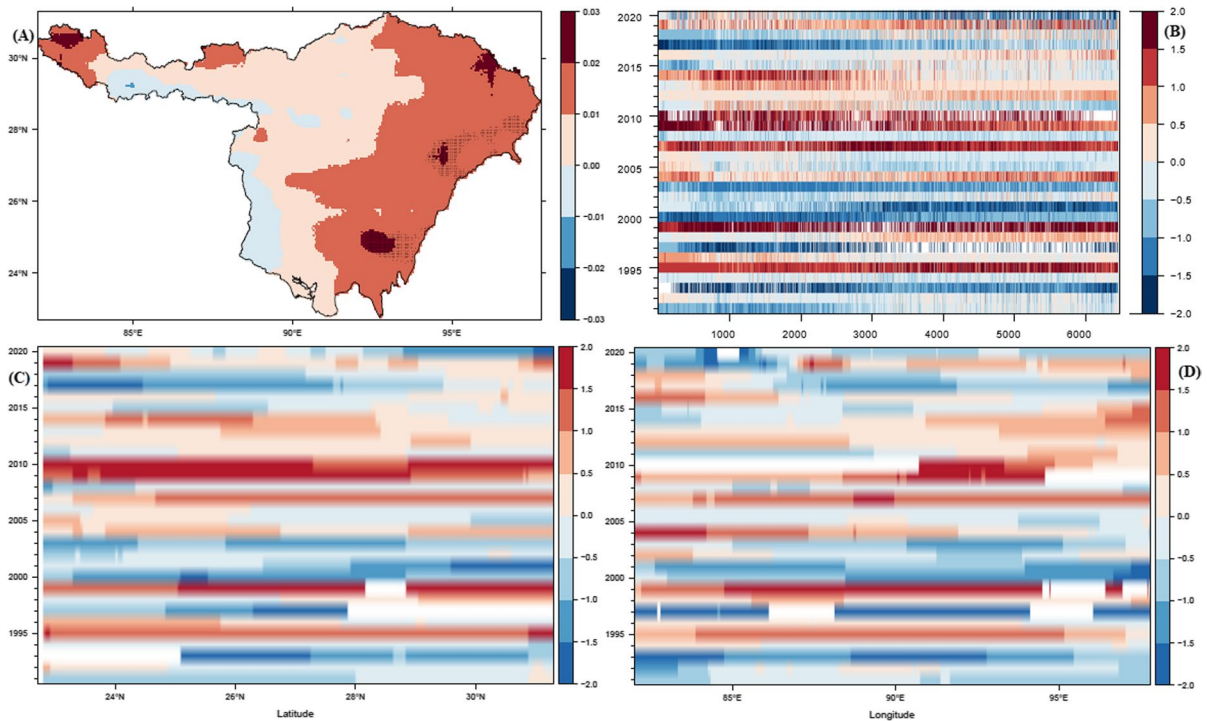


**Fig. 4** Maximum temperature variability over the Brahmaputra basin during the summer season (anomaly map (A) and Hovmoller diagram for altitude (B), latitude (C), and longitude (D), respectively)

middle Ganga plains. However, the recent 2020 data represents a slowing down of the increase in maximum temperature. Interdecadal variability was more prominent during summers where in the first decade (1991–2000), 1995 and 1999 recorded an increase of more than 1 °C, which followed through the years of 2002, 2003, 2004, 2007, and 2009 in the second decade, and 2012, 2016, 2018, and 2019 in the third decade. In recent years, the northern plains of Ganga basin have shown patterns of maximum temperature increase barring 2020.

The maximum temperature anomaly for the Brahmaputra basin was observed between 0.03 and 0.03 °C year<sup>-1</sup> (Fig. 4). A significant temperature increase was found along the south and south eastern margins of the Brahmaputra basin including areas of Nagaland, Mizoram, and Manipur with an anomaly of more than 0.02 °C year<sup>-1</sup>. Only some parts of the basin along its western boundary (Meghalaya and Tripura) have shown a decreasing temperature trend. Some extreme events were observed in the year 1999, 2009, and 2010, where the general temperature increase was more than 1.5 °C. However, with

the help of the Hovmoller plots the major concerning areas can be identified. A fluctuating trend of maximum temperature was observed in the Brahmaputra basin where till 2003 only the years 1995 and 1999 recorded an increase of more than 1 up to 2.0 °C. After 2003, a gradual increase ranging between 0.5 and 2.0 °C was observed till the recent years barring 2011, 2015, 2018, 2019, and 2020. Extreme increases in maximum temperature were observed in the years 1999, 2009, and 2010.

*Minimum temperature over the Ganga–Brahmaputra basin*

The minimum temperature linear trend analysis (Fig. 5) was based on the months of November to February (winter season). The higher altitude region of the Ganga basin has shown a significant increase in the temperature anomaly of the minimum temperature reaching up to 0.04 °C year<sup>-1</sup>, symbolizing the maximum change over the northern part of Ganga basin. Surrounding the maximum increase over the parts of Himachal, Uttarakhand, and adjoining Uttar

Pradesh, the temperature increase was observed in a buffer zone with an increase of 0.02 to 0.03 °C year<sup>-1</sup> in parts of Uttar Pradesh, Delhi, Haryana, and Nepal. The nearby states of Rajasthan, Gujarat, Madhya Pradesh, Bihar, and Nepal recorded an increase of 0.01 to 0.02 °C year<sup>-1</sup>. The lower Ganga plains represent a decrease in the minimum temperature despite being close to the ocean, reflecting the change in the pattern of increase and decrease of temperature over the mountains and plains. The Hovmoller plots extreme change was observed in the year 2005, 2009, 2010, 2017, and 2018, where the increase was recorded more than 2 °C. Whereas, the decrease in the minimum temperature of about -2 °C was observed in the year 1991, 1997, 2014, and 2020. From 1996 to 2010, the minimum temperature across the whole basin started increasing ranging from 0.10 to 2.0 °C. After 2018, the pattern of minimum temperature shows a decreasing trend along the whole basin area.

The minimum temperature trend over the Brahmaputra basin (Fig. 6) represents a major area under the influence of an increase in the temperature with

more than 0.02 °C year<sup>-1</sup>. The significant pixels were observed along the north and north eastern boundary of the basin. The lower Brahmaputra region comprising the area of Manipur, Mizoram, and Tripura shows a decreasing pattern ranging between 0.01 and 0.02 °C year<sup>-1</sup>.

The analysis based on the Hovmoller diagrams represents a clear pattern of climate change after the late 1990. The increasing pattern of the minimum temperature started after the year 2000. Despite the major area of Brahmaputra with high altitude region being covered with forest and receiving high intensity of rainfall, the temperature increase is very prominent. After 2010, a slight change in the trend was observed along the 26° N latitude. The minimum temperature during 1991 to 1998 was observed to be decreasing with temperature ranging between -1 and -2 °C. From 1998 to 2010, the Brahmaputra basin faced sudden temperature increment with a maximum increase of more than 1.5 °C was observed during 1999, 2005, and 2009. 2012 to 2015 was marked with decreasing minimum temperature in the lower Brahmaputra valley lying across 24° N to 28° N and 90° E to 95° E.

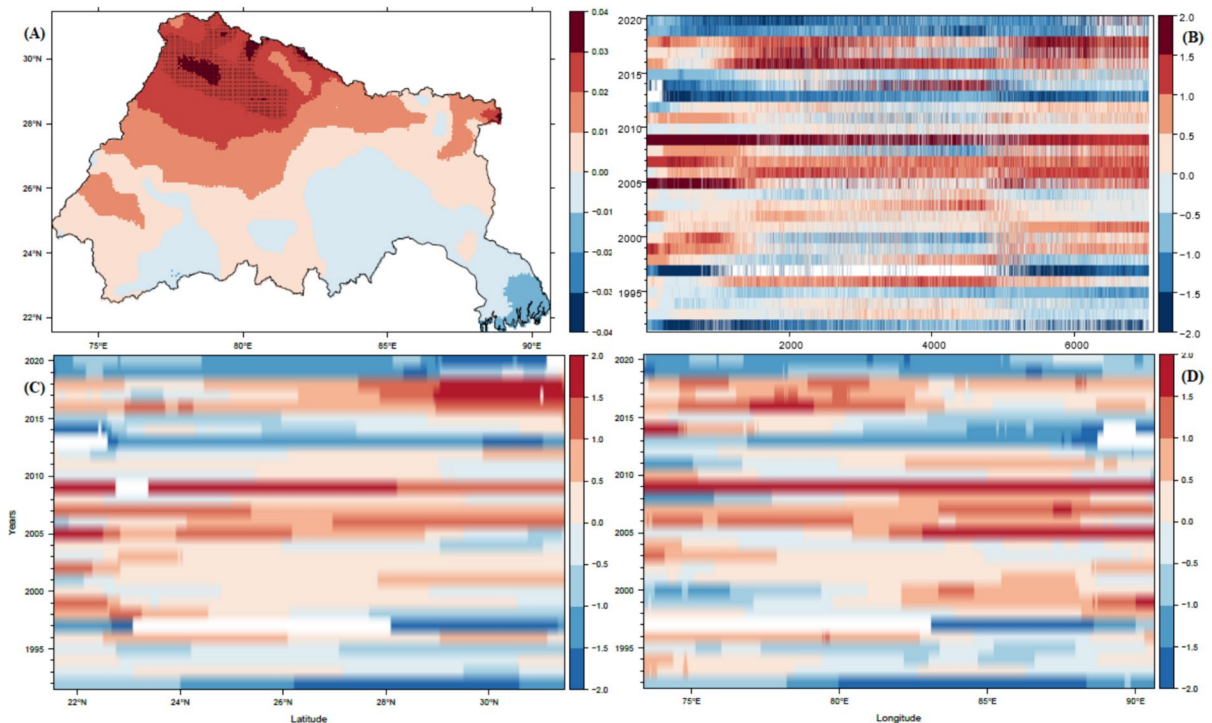


**Fig. 5** Minimum temperature variability over the Ganga basin during the winter season (anomaly map (A) and Hovmoller diagram for altitude (B), latitude (C), and longitude (D), respectively)



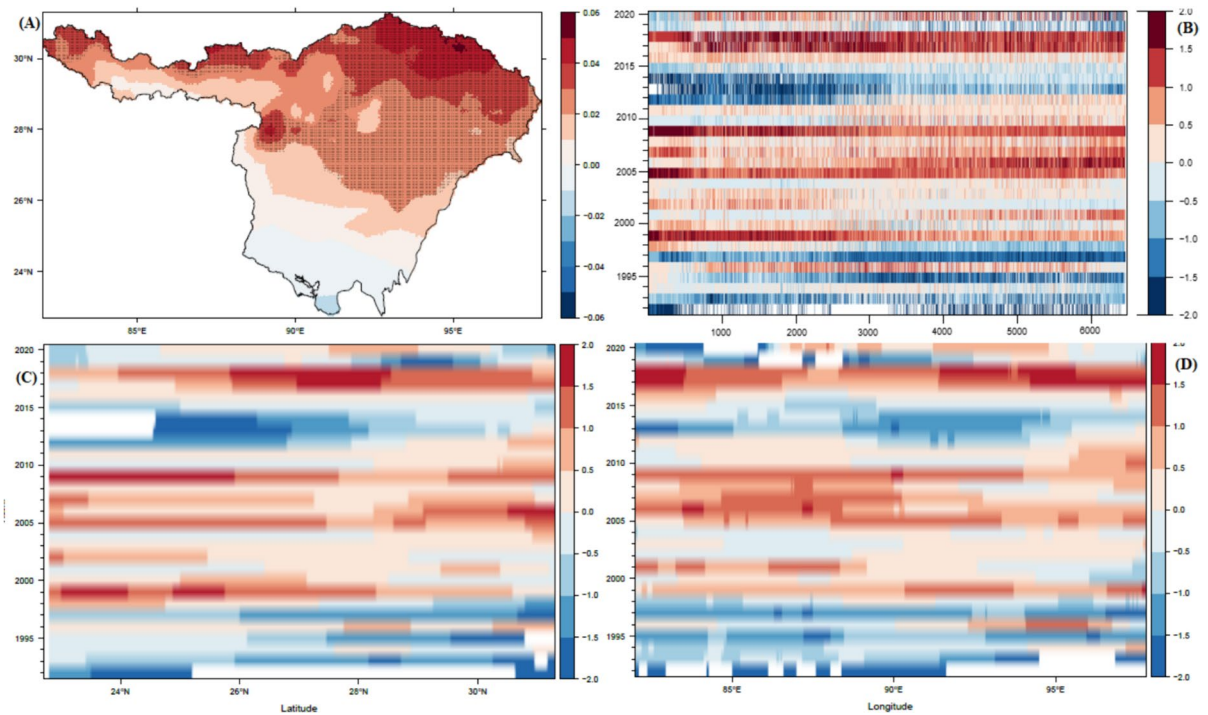


**Fig. 6** Minimum temperature variability over the Brahmaputra basin during the winter season (anomaly map (A) and Hovmoller diagram for altitude (B), latitude (C), and longitude (D), respectively)

After 2015, during 2017 and 2018 minimum temperature began increasing revealing fluctuating climatic patterns across the basin.

A number of variables related to regional climate dynamics and climate change may be responsible for the rise in the maximum and minimum temperature in the Ganga and Brahmaputra basins. The major changes in terms of increasing maximum temperature were observed along the western and eastern boundary of the Ganga and Brahmaputra basin respectively that may challenge the growth cycles of crops and their overall productivity. The northwestern boundary of the Ganga basin is characterized by continental climate and experiences extreme temperature variations, with very hot summers that allows for high heat absorption and retention. Whereas the northeastern boundary of the Brahmaputra basin is typically more humid and influenced by monsoons but can experience significant heat buildup due to the surrounding topography, including hills and valleys, which can trap heat. The specific climatic anomalies and trends in these regions might be influenced by regional factors that can impact wind patterns and moisture

distribution leading to differential heating patterns across different parts of the basins. However, in terms of increment in the minimum temperature, the northern region comprising the Himalayas was majorly affected in the Ganga–Brahmaputra basin. The situation is more alarming for the Brahmaputra basin that can be attributed to the global warming impacts leading to increased absorption of sunlight in the Himalayan region, increasing urbanization, shifts in atmospheric circulations majorly affecting the high-altitude zones.

#### Rainfall variability

Rainfall variability analysis was based on the precipitation data for the months of July to October (Rainy Season) from the year 1991–2020. The rainfall trend shows the current reversed situation of the Ganga and Brahmaputra basin. The lower Ganga basin including the states of Bihar, Jharkhand, and some parts of Uttar Pradesh, Madhya Pradesh, and Nepal represents an increased rainfall anomaly of 1–3 mm year<sup>-1</sup> (Fig. 7). The maximum increase of more than 2.5 mm year<sup>-1</sup>

was observed in Rajasthan. The central Ganga basin comprising the states of Delhi, Haryana, Uttar Pradesh, and Uttarakhand records a decreasing anomaly ranging between  $-0.5$  and  $-2$  mm year $^{-1}$ .

The anomaly increase of rainfall is prominent in the Ganga basin; however, based on the Hovmoller plots it was observed that the increase was a result of the recent years from 2012 to 2020. The major years where the increase was observed were 1995, 1999, 2005–2007, 2014–2016, and 2019. The region saw drier circumstances in the first decade (1991–2000), which had slightly improved by the end of 1997 until 2000. The region saw its worst conditions in the second decade (2001–2010), with a decrease of more than  $-2$  mm year $^{-1}$ , which was later improved in the third decade (2011–2020).

The pixels with 90% significance level along the Brahmaputra basin (Fig. 8) were found on the decreasing pattern of rainfall along the parts of Assam, Arunachal Pradesh, and Nagaland with a decrease of

more than  $-1$  to  $-2.5$  mm year $^{-1}$ . The basin generally receives an annual average rainfall of about 2500 mm but during the recent time, it has been showing clear impacts of climate change with its decreasing pattern of rainfall. The trend of rainfall intensity of the Himalayan region in the Brahmaputra basin remains moreover constant. The only increase in the rainfall anomaly of about  $2$ – $3$  mm year $^{-1}$  was observed in parts of Meghalaya, Mizoram, and Tripura.

The Hovmoller diagrams represent a fluctuating trend of the increase and decrease of precipitation, with a very slight increase in the rainfall intensity over the basin in the recent years. The years where the increase of more than  $2$  mm year $^{-1}$  was observed were 1991, 1998–1999, 2007, 2011, 2013, 2015, and 2017, whereas a prominent decrease of more than  $-1.5$  was evident in 1993–1994, 2004–2006, 2014, and 2018.

The Ganga basin comprising the plains and plateau regions of the country, receiving lower rainfall intensity as compared to the Brahmaputra basin having an

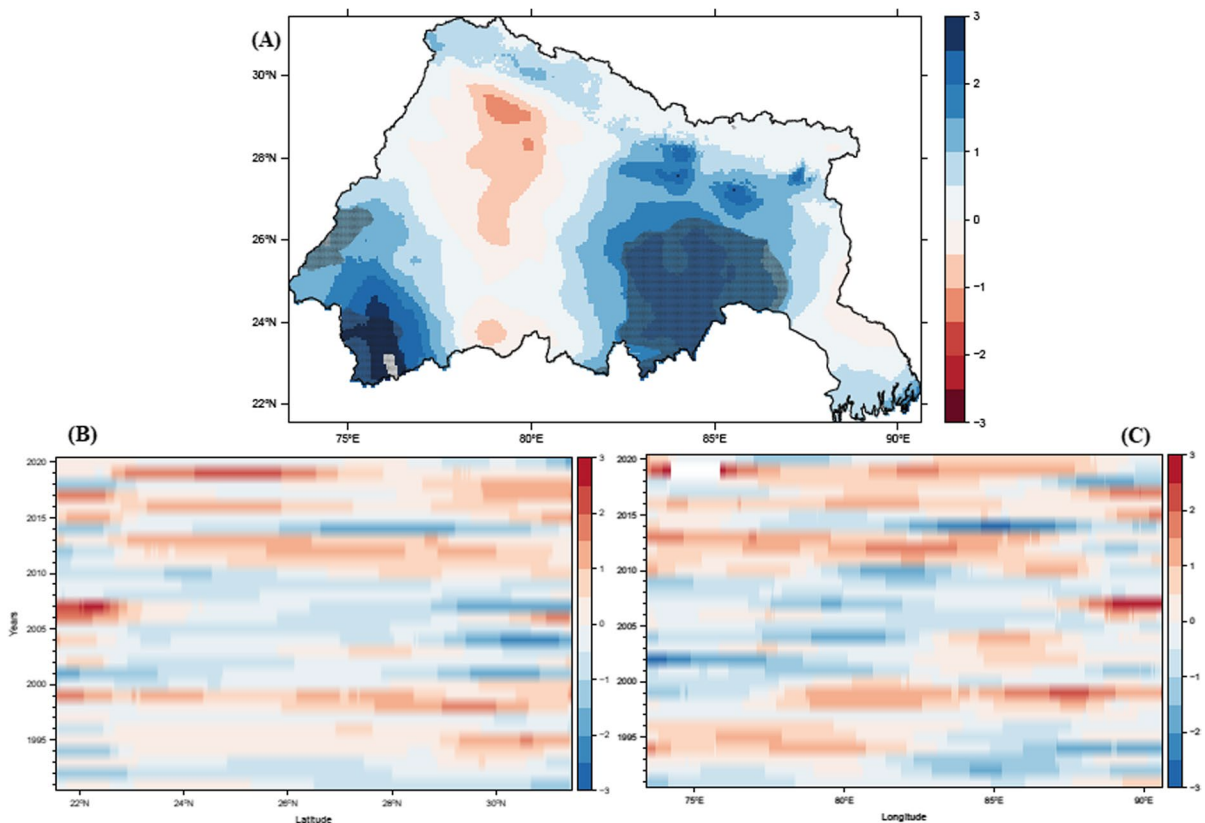


**Fig. 7** Rainfall variability over the Ganga basin during the monsoon season (anomaly map (A) and Hovmoller diagram for latitude (B) and longitude (C))

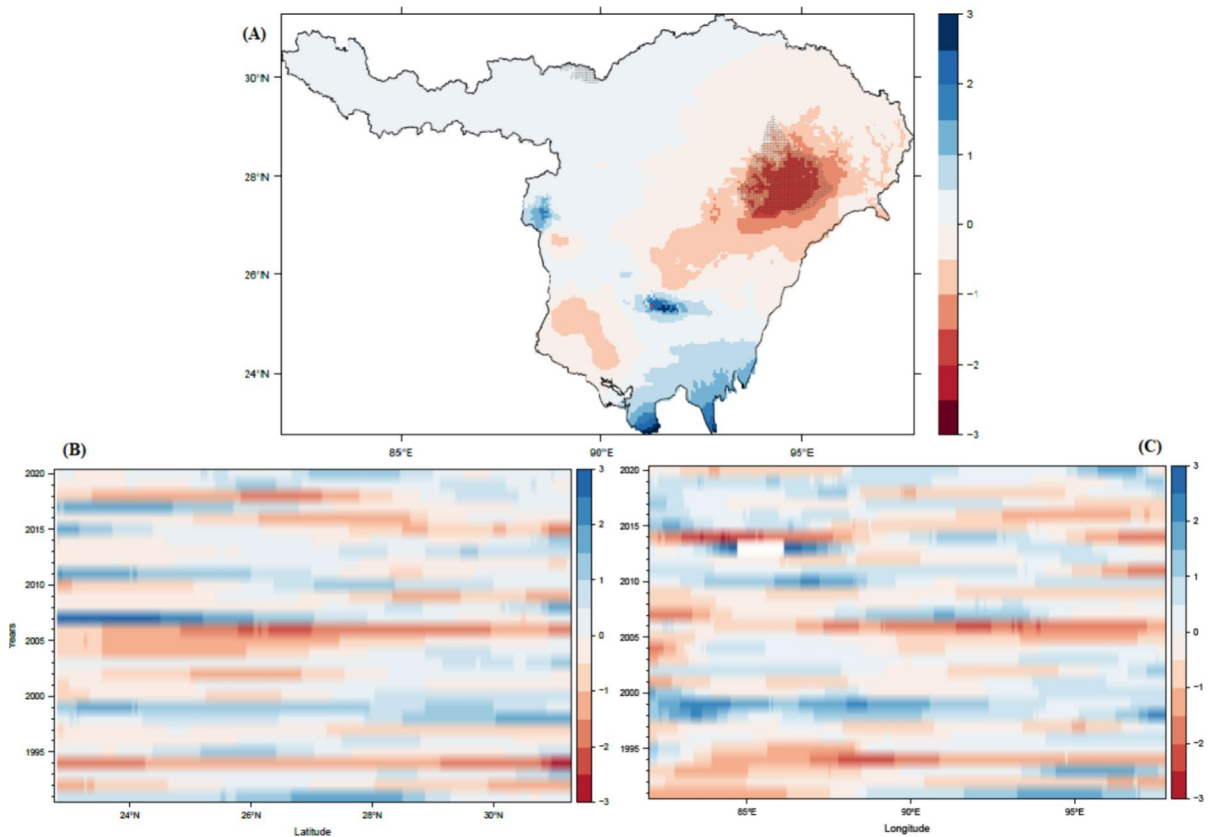


**Fig. 8** Rainfall variability over the Brahmaputra basin during the monsoon season (anomaly map (A) and Hovmoller diagram for latitude (B) and longitude (C))

extensive forest cover has shown an increasing rainfall anomaly of more than 2 mm year<sup>-1</sup>. The Hovmoller representation of the Ganga and Brahmaputra basin reveals distinct patterns, with the Ganga basin witnessing decadal variations in rainfall and the Brahmaputra basin experiencing irregular rainfall. Based on the priority areas in terms of increased temperature and decreased rainfall Policymakers and stakeholders can utilize these insights to develop more resilient infrastructure and mitigate the impacts of climate change on communities and ecosystems by using early warning systems, developing resilient infrastructure, promote sustainable water management practices, restoring natural ecosystems, and foster community participation.

#### Standardized Precipitation Index

Standardized Precipitation Index is widely used for the analysis of drought occurrences, whereas it can

also be used for the identification of the wet periods. Dry and wet periods along the basins will provide better insight on its changing characteristics and pattern (Fig. 9). The SPI generated for Ganga basin for the year 1991–2000 and 2011–2020 recorded fewer extreme events and high fluctuations were observed during the decade of 2001–2010 due to the presence of many drought extremes. Whereas along the Brahmaputra basin no such extremes (flood or drought) were recorded as the SPI values were only fluctuating under the range of -1 to 1. Based on the analysis of wet and dry periods over the time period of 1991–2020 it was observed that the chances of floods or wet years are more in comparison to dry years in the Ganga basin with an occurrence of 25:20 and vice versa in the Brahmaputra basin with an occurrence of 17:16 respectively (Table 2) as a regular pattern of dry spells was observed for the Brahmaputra basin. The wet spell for both the Ganga–Brahmaputra

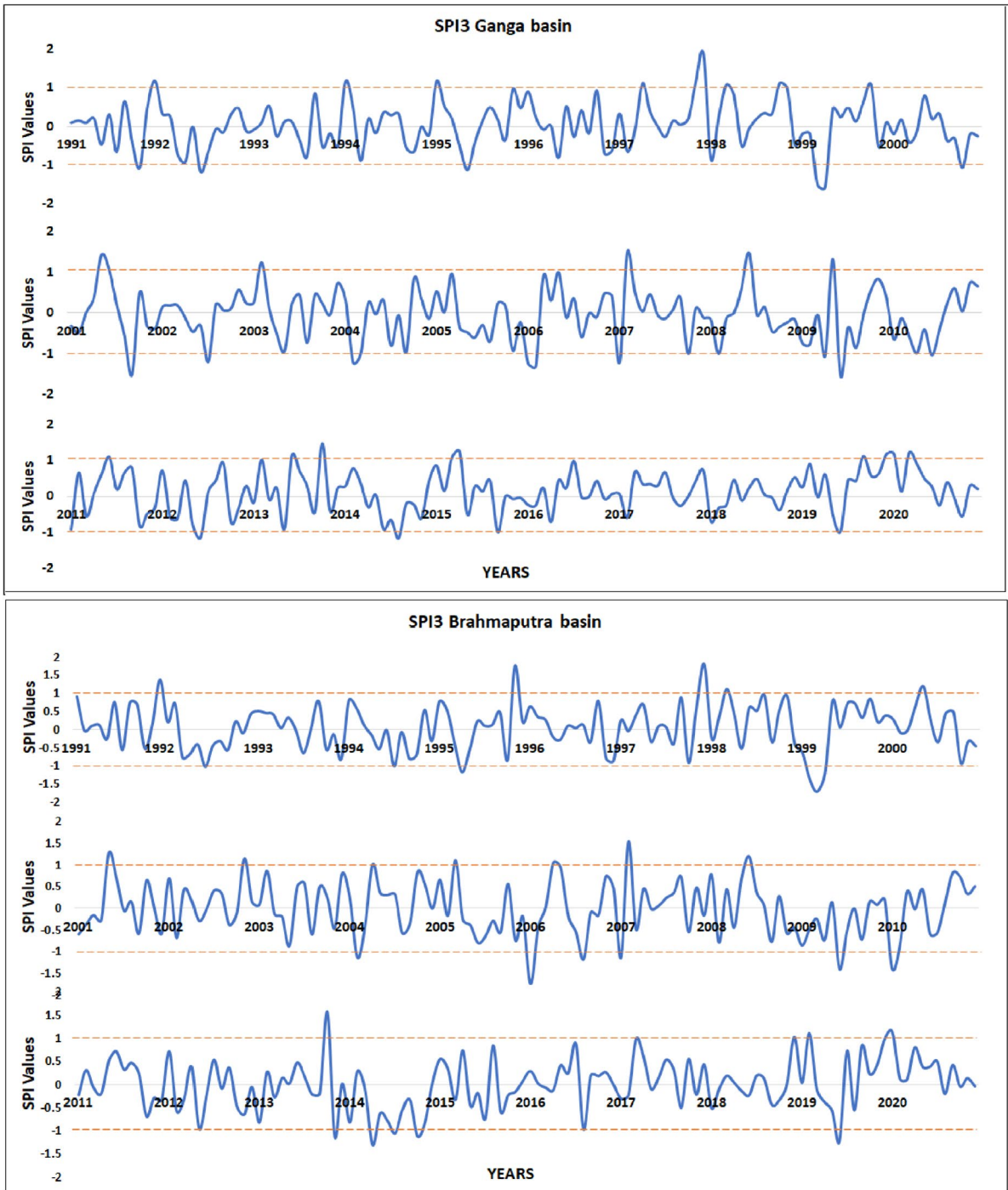


**Fig. 9** SPI3 values for Ganga–Brahmaputra basin (30 years)

basin are generally higher. The wet and dry period analysis increases concerning the pattern of change for the Ganga–Brahmaputra basin, as Ganga basin

is more prone to drought events due to its large area confining different topography (from Himalayas to deserts and alluvial plains) but is showing instances

of abnormally high wet spells. Whereas, the Brahmaputra basin despite receiving high-intensity rainfall has shown a declining precipitation trend over the last decade of 2011–2020 as more occurrences of dry spells were found in the basin. It was observed that the Ganga–Brahmaputra basin together is showing more prominent extremes of dry spells.

Global oscillations

The correlation analysis between SPI3 and Niño 3.4 for the Ganga basin provided a negligible positive relationship between the indices (median  $r=0.19$ ) (Fig. 10). Whereas, the Brahmaputra basin has provided a negative correlation (median  $r= -0.32$ ) over the past 30 years. The distinctive climatic and geographic factors in the Ganga and Brahmaputra basins can account for the varying relationships between the Niño 3.4 index and the Standardized Precipitation Index (SPI). During El Niño events there is a weakening of the monsoon winds, however, due to increased frequency of low-pressure systems or cyclonic

activity in the Bay of Bengal can bring significant rainfall to the Ganga basin resulting in a positive correlation. Whereas the Brahmaputra basin is directly affected by the primary monsoon currents.

Cross-correlation was applied to understand the deviation of the correlation values among the variables using the lag information (Fig. 11). The highest correlation in the Ganga basin was recorded at lag 1, based on the lag 1 correlation, variable (Niño 3.4) is correlated with the preceding value of SPI3. In particular, this lag 1 connection shows that variations in this month’s Niño 3.4 index are correlated with variations in the SPI3 values of the next month. The highest correlation in the Brahmaputra basin was recorded at lag –1 (median  $r= -0.382$ ). The result highlights distinct climatic responses in the Ganga and Brahmaputra areas and aids in understanding the time-lag impacts of El Niño conditions on precipitation patterns in these two basins.

The correlation between monsoonal SPI3 and Niño 3.4 (Fig. 12) represents a negative relationship for Ganga–Brahmaputra basin concluding that if the Niño 3.4 value will increase (presenting El Niño if the values exceed +0.4C), the corresponding SPI3 values will decrease (decreased SPI3 values represents drought conditions). The summer and winter seasons have shown a positive correlation in Ganga–Brahmaputra basin, where the highest correlation is found in winters (Ganga basin ( $r=0.47$ ), Brahmaputra basin ( $r=0.56$ )). Niño 3.4 only considers SSTs, and no other atmospheric variables that are used to characterize the behaviors of an El Niño or a La Niña occurrence adding to

**Table 2** Wet and dry period estimated using SPI

| Year      | Wet period |             | Dry period |             |
|-----------|------------|-------------|------------|-------------|
|           | Ganga      | Brahmaputra | Ganga      | Brahmaputra |
| 1991–2000 | 9          | 5           | 6          | 6           |
| 2001–2010 | 6          | 7           | 12         | 6           |
| 2011–2020 | 10         | 4           | 2          | 5           |

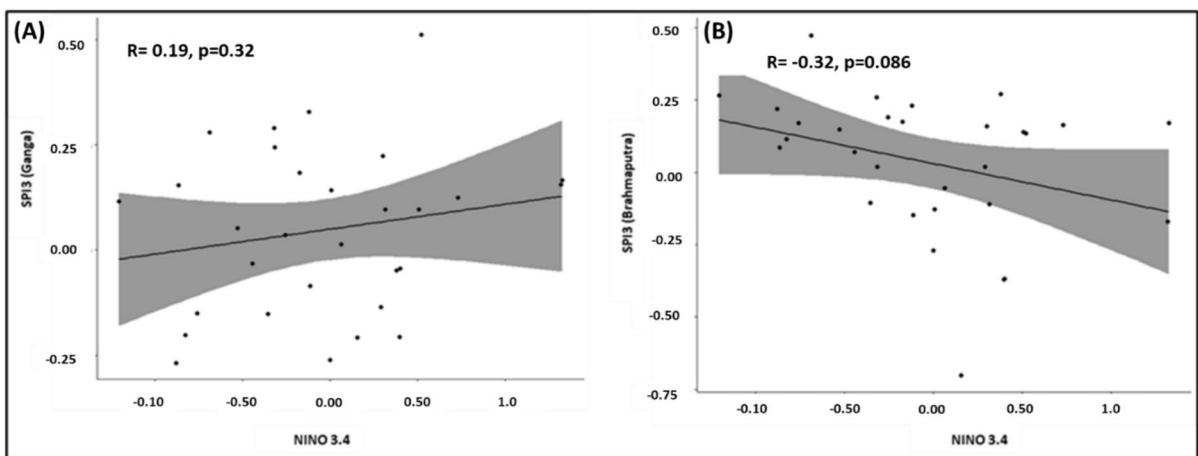


**Fig. 10** Correlation between Niño 3.4 and SPI3 over Ganga (A) Brahmaputra (B) basin

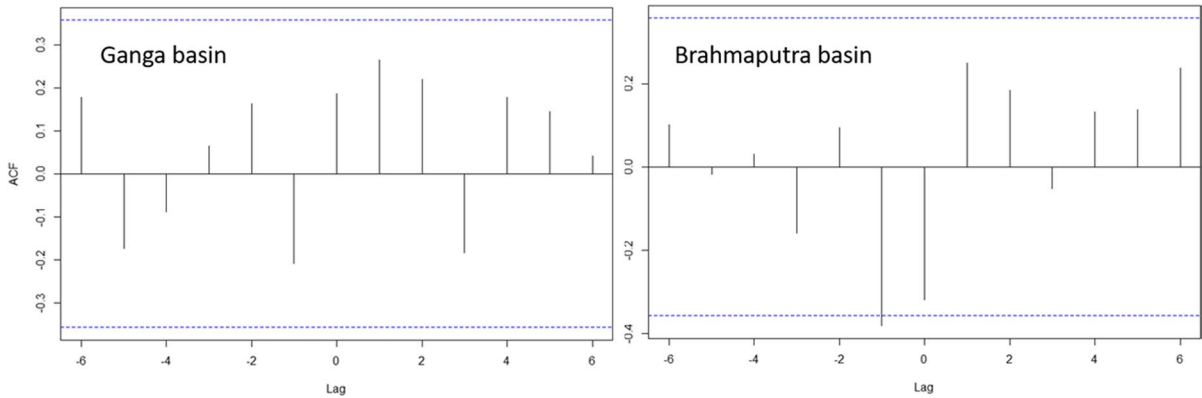


**Fig. 11** Cross correlation over GB basin between Niño 3.4 and SPI3 on lag6

some limitations to accurately justifying the relation between the regional and global oscillations.

**Discussion**

The Ganga–Brahmaputra basin is highly influenced by the fast-changing climate, with recurring floods and flash droughts affecting vast area of the basin.

Based on the linear trend analysis, the maximum and minimum temperature revealed a maximum anomaly increase of 0.06 °C and 0.04 °C respectively over the Ganga basin, and 0.03 °C and 0.06 °C over the Brahmaputra basin. The parts of the basin even recorded an increase of more than 1.5 °C year<sup>-1</sup>. Most of the results obtained are in conformity with previous studies, the pattern of temperature (1950–1989) over the upper and middle parts of the Ganga basin represents

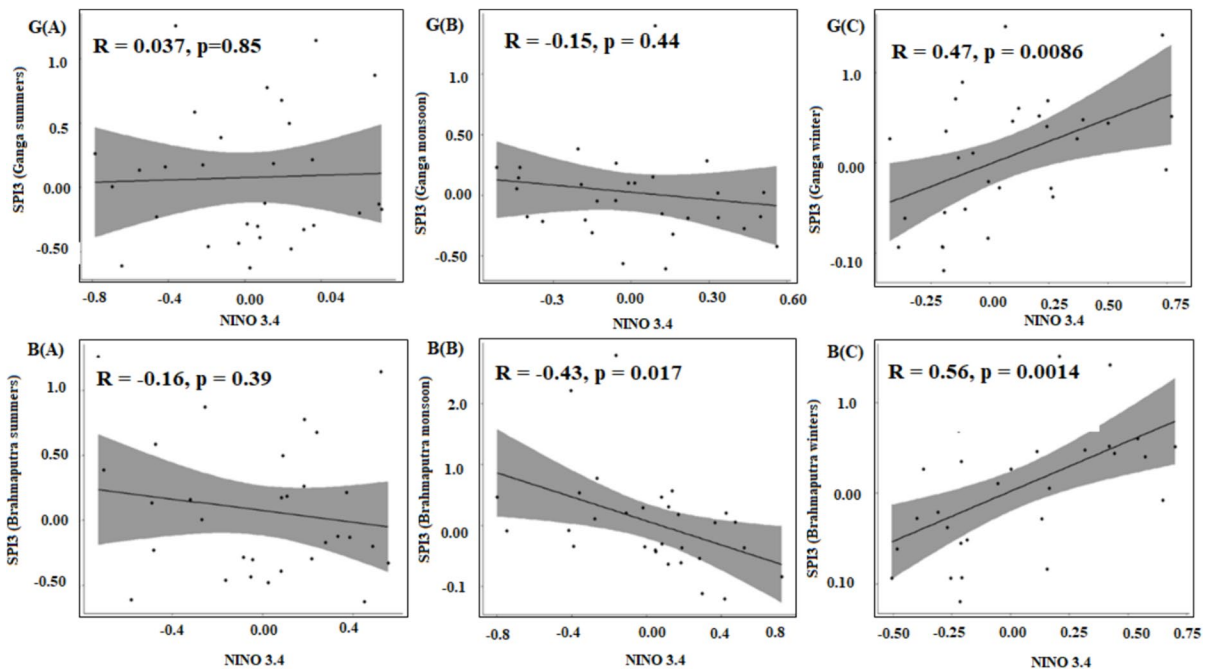


**Fig. 12** Seasonal correlation analysis over Ganga (G)-Brahmaputra (B) basin between Niño 3.4 and SPI3, for summers (G(A) and B(A)), monsoon (G(B) and B(B)), and winters (G(C) and B(C))

that the annual maximum temperature in the basin is on the rise (Kothyari et al., 1997). Over the past 101 years from 1901 to 2002, the mean, maximum, and minimum temperature in the Upper Ganga basin has increased by 0.60 °C, 0.60 °C, and 0.62 °C, respectively (Mishra et al., 2014). Based on various temperature trend studies, the minimum and maximum temperature increase was evident for the Brahmaputra basin. The greatest increase in the trend during the period of 1961–2005 in the upper Brahmaputra river basin was found in the winter season with +0.37 °C/decade which is a little more than in fall +0.35 °C/decade. For the summer and spring seasons, an increasing trend of +0.17 °C and +0.27 °C/decade has been defined (Bongartz et al., 2007). Based on the analysis of climatic research unit data for the year 1900–2002, it was observed that a temperature increase of 0.6 °C per 100 years showed a higher increase in the spring season (Immerzeel, 2008). Based on different climate change scenarios and climate model COSMO-CLM, an increase in temperature in the Brahmaputra basin for all seasons was observed and the highest values were recorded over the Tibetan plateau (Dobler et al., 2011). These models and projections are based on scenarios that consider continued greenhouse gas emissions, indicating ongoing and future warming.

The rainfall anomaly-based trend analysis attempted in the present study provides a significant positive trend in the Ganga basin (2.5 to 3 mm year<sup>-1</sup>) and a negative trend in the Brahmaputra basin. During the recent years (1988–2017), it was observed that the rainfall trend was decreasing over the Brahmaputra basin whereas the Ganga basin recorded a non-significant trend because of a complex pattern (Patel et al., 2021). The Climate model scenarios representing the 1.5° and 2 °C warming level over the Ganga–Brahmaputra basin revealed an increase in extreme precipitation (Uhe et al., 2019).

Standardized Precipitation Index has been widely used for the identification of flood and drought occurrences. The major flood years observed based on the SPI3 in the Ganga basin were 1992, 1994, 1995, 1998, 2001, 2003, 2007–2009, 2013–2015, and 2020, which are in line with flood-related studies in the basin. In the year 2020, Bihar and West Bengal were majorly flood-affected (Pandey et al., 2022) that had a recurrent inundation for Bihar in the year 2021 as a result of high-intensity rainfall over the Himalayan

region (Kaushik et al., 2022). Findings suggest of major disasters occurring in 2007 and 2020 in North Bihar (Tripathi et al., 2022), and in 2008 in Kosi watershed (Singh et al., 2011) due to its dynamic nature (Bhatt et al., 2010). In the Bansloi river catchment, the most destructive floods were experienced in 1995, 2000, 2004, and 2007 (Paul et al., 2019). The historical significant flood events in the North Bihar region were identified during 1995, 1998, 2000, 2001, 2003, 2004, 2008, 2010, 2013, 2016, 2017, and 2018 (Tripathi et al., 2020). Extensive flood occurrences in West Bengal were in the years 1995, 1999, 2000, 2006, 2007, and 2008 (Ghosh & Kar, 2018; Samal et al., 2014).

The flood occurrences in the Brahmaputra basin have been very prominent because of higher intensity rainfall in the North Eastern States of India, impacting the vast area in Bangladesh due to increased runoff which leads to extensive loss of economy. The flood years observed in our study (1992, 1996, 1998, 2001, 2007, 2008, 2013, 2019, and 2020) based on SPI3 values are backed up with historical and present studies. In a recent study, the area under flood inundation in the monsoon season was estimated to be 25,889.1 km<sup>2</sup> for Bangladesh and 13,460.1 km<sup>2</sup> for Assam (Pandey et al., 2022). One of the extreme flood events was observed in 1998 with the highest flood level of 106.41 m near Dibrugarh (Dhar and Nandargi, 2000) with other major flood events of 1998, 2013, 2019, and 2020 in Assam. Over the parts of Bangladesh, floods of 1998, 2007, 2019, and 2020 have damaged vast areas (Samal et al., 2014). During the recent years, the occurrences of floods have been increasing on a vast scale, affecting major agriculturally important zones of Ganga–Brahmaputra basin.

The major drought occurrences based on the SPI3 were observed in the years 1995, 1999, 2001, 2002, 2004, 2006, 2009, 2010, 2013, 2014, 2015, and 2019 in Ganga–Brahmaputra basin. The frequency of drought events has been severe after 1965, there were 12 occurrences of extreme drought events in the Ganga basin, out of which drought cases of 2002 and 2009 were considered severe (Banerjee & Pandey, 2021). In the Brahmaputra basin, the drought of 2014–2015 was one of the longest drought observed (Dharpure et al., 2022). The whole basin recorded significantly low precipitation in 1999, 2006, and 2009 where major portion of the basin was under the influence of drought (Parajuli et al., 2021).

The spatial and seasonal response of the precipitation in the basin has been modulated by ENSO and Indian Ocean Dipole. During the El Niño event there is deficit in precipitation in western west Bengal, Arunachal Pradesh, western part of Assam, northern west Bengal, and northern Bangladesh and the most precipitation is on the occurrence of La Niña and a negative IOD (Pervez & Henebry, 2015). The variability of Indian monsoon based on the influence of ENSO has been studied by several authors, and the relationship has been difficult to replicate (Webster et al., 1998). Based on the correlation statistics, a positive correlation was found between meteorological drought and Niño 3.4 SST over the districts of northern, central, and peninsular India, while the north eastern districts recorded a negative correlation (Guhathakurta et al., 2017). The present study revealed a non-significant negative correlation between the Niño 3.4 and SPI during the monsoon season. The same has been observed while correlating IODs, SST, and Niño 3.4 with SPI that Niño 3.4 significantly negatively affects SPI. If Niño 3.4 increases (decreases), the SPI drops (increases) considerably leading to more drought (wet) conditions (Yadav et al., 2023). There is a well-known inverse relationship between ENSO and rainfall, leading to higher (/lower) rainfall in periods of lower (/higher) ENSO indices (Narasimha & Bhattacharyya, 2010). The strongest El Niño years recorded in the past are of 1982–1983, 1997–1998, and 2014 and 2015 (Lv et al., 2022). The temperature increase during the El Niño years is very prominent in the Ganga Brahmaputra basin that increases the frequency and impacts of drought. A maximum correlation occurring at  $-1$  lag implies that the “ $x$ ” variable leads the “ $y$ ” variable that is the precursor of a cause-effect relationship (Munagapati and Tiwari, 2021) that was observed with Brahmaputra basin in the present analysis. Drought analysis based on optical datasets has been widely used previously; however, there is limited understanding of the use of microwave data in spatiotemporal drought studies.

Some other potential limitation of the study lies in the non-availability of rainfall datasets in the hilly regions of North East India and China due to limitations of gauging stations and the potential uncertainties and limitations of the climate data. The future studies can focus on other advanced statistical or machine learning methods that could provide deeper

insights by including other climatic variables such as humidity, wind patterns, or soil moisture, which can significantly impact the region’s climate and agricultural output.

## Conclusion

The present study illustrates the changing pattern of climate over the past 30 years (1991–2020) in the Ganga–Brahmaputra basin using anomaly analysis that provides a holistic aspect of the study with the help of Hovmoller diagrams to better understand the changing climate over different latitude, longitude, and altitude. The linear trend analysis of the basin reveals changing situations of Ganga and Brahmaputra basin over the recent years. The maximum temperature anomaly increase was found to be more than  $0.05\text{ }^{\circ}\text{C year}^{-1}$  in the Ganga basin and  $0.03\text{ }^{\circ}\text{C year}^{-1}$  in the Brahmaputra basin depicting an overall increase in the maximum temperature in the recent years. The same pattern of increase was found in the minimum temperature anomaly, with an anomaly increase of  $0.04\text{ }^{\circ}\text{C year}^{-1}$  and  $0.06\text{ }^{\circ}\text{C year}^{-1}$  in the Ganga–Brahmaputra basin, respectively. The increase in minimum temperature was more prominent in the Brahmaputra basin. The precipitation trend presents a different scenario of the basin than what was previously thought as considerable for GB basin where positive trends ( $+3\text{ mm year}^{-1}$ ) were observed in some areas of the Ganga basin, whereas significant negative trends ( $-3\text{ mm year}^{-1}$ ) predominated in the Brahmaputra basin. The wet and dry period estimation based on the SPI values more than  $+1$  and less than  $-1$  respectively revealed an occurrence of 25:20 for the Ganga basin concluding increased flood occurrences and an occurrence of 16:17 was observed over the Brahmaputra basin presenting an increased drier condition depicting the vulnerability of the GB basin to both natural disasters. Where excessive rainfall can saturate the soil, causing waterlogging, damaging crops, and delaying planting or harvesting activities whereas drier conditions will lead to crop failure, livestock shortages, and increased competition for water resources, impacting the overall agricultural output. The present work will be useful for the mitigation of climate change impacts on the Ganga–Brahmaputra basin, the major food belt of India.



**Acknowledgements** The authors acknowledge the United States Geological Survey (USGS) for making the MODIS (LULC) data freely available that was used in the present study. The author would like to acknowledge Climatology Lab for making TerraClimate data (precipitation and temperature) available. The author wish to the Global Climate Observing System, Working Group on Surface Pressure for making the Nino 3.4 data available.

**Author contributions** Kavita Kaushik: conception and design, acquisition of data, analysis and interpretation of data, writing—original draft.

Arvind Chandra Pandey: conception and design, writing—review and editing, supervision, final approval of the version.

Chandra Shekhar Dwivedi: writing—review and editing.

**Funding** The authors declare that no funds, grants, or other support were received during the preparation of this manuscript.

**Data availability** Data will be made available on request.

**Declarations**

**Competing interests** The authors declare no competing interests.

## References

- Ahmed, N. (2022). *Ganges river—climate and hydrology* | *Britannica*. Britannica. <https://www.britannica.com/place/Ganges-River>. Accessed 23 Jul 2023
- Abatzoglou, J. T., Dobrowski, S. Z., Parks, S. A., & Hegewisch, K. C. (2018). TerraClimate, a high-resolution global dataset of monthly climate and climatic water balance from 1958–2015. *Scientific Data*, 5(1), 1. <https://doi.org/10.1038/sdata.2017.191>
- Alam, N. M., Sharma, G. C., Moreira, E., Jana, C., Mishra, P. K., Sharma, N. K., & Mandal, D. (2017). Evaluation of drought using SPEI drought class transitions and log-linear models for different agro-ecological regions of India. *Physics and Chemistry of the Earth, Parts a/b/c*, 100, 31–43. <https://doi.org/10.1016/j.pce.2017.02.008>
- Apurv, T., Mehrotra, R., Sharma, A., Goyal, M. K., & Dutta, S. (2015). Impact of climate change on floods in the Brahmaputra basin using CMIP5 decadal predictions. *Journal of Hydrology*, 527, 281–291. <https://doi.org/10.1016/j.jhydrol.2015.04.056>
- Banerjee, S., & Pandey, A. C. (2021). Catchment-level agricultural drought hazard vulnerability analysis of Ganga Basin (India) using spectral indices. *Arabian Journal of Geosciences*, 14(17), 1782. <https://doi.org/10.1007/s12517-021-07825-6>
- Bar, S., Parida, B. R., Roberts, G., Pandey, A. C., Acharya, P., & Dash, J. (2021). Spatio-temporal characterization of landscape fire in relation to anthropogenic activity and climatic variability over the Western Himalaya, India. *Giscience & Remote Sensing*, 58(2), 281–299. <https://doi.org/10.1080/15481603.2021.1879495>
- Barman, S., & Bhattacharjya, R. K. (2015). Change in snow cover area of Brahmaputra river basin and its sensitivity to temperature. *Environmental Systems Research*, 4(1). <https://doi.org/10.1186/s40068-015-0043-0>
- Bhatt, C. M., Srinivasa Rao, G., Manjushree, P., & Bhanumurthy, V. (2010). Space based disaster management of 2008 Kosi floods, North Bihar, India. *Journal of the Indian Society of Remote Sensing*, 38(1), 99–108. <https://doi.org/10.1007/s12524-010-0015-9>
- Bhunia, P., Das, P., & Maiti, R. (2020). Meteorological drought study through SPI in three drought prone districts of West Bengal, India. *Earth Systems and Environment*, 4(1), 43–55. <https://doi.org/10.1007/s41748-019-00137-6>
- Bongartz, K., Flügel, W. A., Pechstädt, J., Jiangchu, X., & Yao, T. (2007). Analysis of climate change trend and possible impacts in the upper Brahmaputra river basin—The BRAHMATWINN Project. *MODSIM07 - landwater and environmental management: Integrated systems for sustainability, proceedings, Ives, 2004* (pp. 2124–2130). [https://www.iwra.org/congress/2008/resource/authors/abs435\\_article.pdf](https://www.iwra.org/congress/2008/resource/authors/abs435_article.pdf). Accessed 1 June 2023
- Chowdhury, M. D. R., & Ward, N. (2004). Hydro-meteorological variability in the greater Ganges–Brahmaputra–Meghna basins. *International Journal of Climatology*, 24(12), 1495–1508. <https://doi.org/10.1002/joc.1076>
- Das, J., Gayen, A., Saha, P., & Bhattacharya, S. K. (2020). Meteorological drought analysis using Standardized Precipitation Index over Luni River basin in Rajasthan, India. *SN Applied Sciences*, 2(9), 1530. <https://doi.org/10.1007/s42452-020-03321-w>
- Dhar, O. N., & Nandargi, S. (2000). A study of floods in the Brahmaputra basin in India. *International Journal of Climatology*, 20(7), 771–781. [https://doi.org/10.1002/1097-0088\(20000615\)20:7%3c771::AID-JOC518%3e3.0.CO;2-Z](https://doi.org/10.1002/1097-0088(20000615)20:7%3c771::AID-JOC518%3e3.0.CO;2-Z)
- Dharpure, J. K., Goswami, A., Patel, A., Kulkarni, A. V., & Meloth, T. (2022). Drought characterization using the combined terrestrial evapotranspiration index over the Indus, Ganga and Brahmaputra river basins. *Geocarto International*, 37(4), 1059–1083. <https://doi.org/10.1080/10106049.2020.1756462>
- Dobler, A., Yaoming, M., Sharma, N., Kienberger, S., & Ahrens, B. (2011). Regional climate projections in two alpine river basins: Upper Danube and Upper Brahmaputra. *Advances in Science and Research*, 7(1), 11–20. <https://doi.org/10.5194/asr-7-11-2011>
- Earth Resources Observation And Science (EROS) Center. (2017). *Shuttle Radar Topography Mission (SRTM) 1 Arc-Second Global* [Tiff]. U.S. Geological Survey. <https://doi.org/10.5066/F7PR7TFT>
- Edwards, D. C., & Mckee, T. B. (1997). *Characteristics of 20th century drought in the United States at multiple time scales*. (Climatology Report 97–2). Department of Atmospheric Science, Colorado State University. [https://mountainscholar.org/bitstream/handle/10217/170176/CLMR\\_Climatology97-2.pdf](https://mountainscholar.org/bitstream/handle/10217/170176/CLMR_Climatology97-2.pdf). Accessed 5 Dec 2023
- Fhong, N. Z. (2021). *Delineation of flood inundation extent as the result of land use changes* [Universiti Malaysia Pahang].

- <http://umpir.ump.edu.my/id/eprint/35258/1/>. Accessed 23 Jul 2023
- Gain, A. K., & Giupponi, C. (2014). Impact of the Farakka dam on thresholds of the hydrologic flow regime in the lower Ganges river basin (Bangladesh). *Water*, 6(8), 8. <https://doi.org/10.3390/w6082501>
- Ghosh, A., & Kar, S. K. (2018). Application of analytical hierarchy process (AHP) for flood risk assessment: A case study in Malda district of West Bengal, India. *Natural Hazards*, 94(1), 349–368. <https://doi.org/10.1007/s11069-018-3392-y>
- Guhathakurta, P., Menon, P., Inkane, P. M., Krishnan, U., & Sable, S. T. (2017). Trends and variability of meteorological drought over the districts of India using Standardized Precipitation Index. *Journal of Earth System Science*, 126(8), 120. <https://doi.org/10.1007/s12040-017-0896-x>
- Immerzeel, W. (2008). Historical trends and future predictions of climate variability in the Brahmaputra basin. *International Journal of Climatology*, 2029, 2011–2029. <https://doi.org/10.1002/joc>
- Irawan, A. N. R., Komori, D., & Hendrawan, V. S. A. (2023). Correlation analysis of agricultural drought risk on wet farming crop and meteorological drought index in the tropical-humid region. *Theoretical and Applied Climatology*, 153(1), 227–240. <https://doi.org/10.1007/s00704-023-04461-w>
- Kaushik, K., Pandey, A., Parida, B., and Kumar, N. (2022) Flood monitoring and assessment over the Himalayan River catchment. In B. Parida, A. Pandey, M. D. Behera, & N. Kumar (Eds.), *Handbook of himalayan ecosystems and sustainability*, volume 2: Spatio-temporal monitoring of water resources and climate (pp. 69–84). CRC Press Taylor & Francis Group. <https://doi.org/10.1201/9781003265160-6>
- Komuscu, A. U. (1999). Using the SPI to analyze spatial and temporal patterns of drought in Turkey. 11(1). <https://digit.alcommons.unl.edu/cgi/viewcontent.cgi?article=1048&context=droughtnetnews>. Accessed 15 Mar 2023
- Kothiyari, U. C., Singh, V. P., & Aravamathan, V. (1997). An investigation of changes in rainfall and temperature regimes of the Ganga Basin in India. *Water Resources Management*, 11, 17–34.
- Loaiza Cerón, W., Carvajal-Escobar, Y., Andreoli de Souza, R. V., Toshie Kayano, M., González López, N. (2020). Spatio-temporal analysis of the droughts in Cali, Colombia and their primary relationships with the El Niño-Southern Oscillation (ENSO) between 1971 and 2011. *Atmósfera*, 33(1), 51–69. <https://doi.org/10.20937/atm.52639>
- Lv, A., Fan, L., & Zhang, W. (2022). Impact of ENSO events on droughts in China. *Atmosphere*, 13(11), 11. <https://doi.org/10.3390/atmos13111764>
- Mahmood, R., Jia, S., & Zhu, W. (2019). Analysis of climate variability, trends, and prediction in the most active parts of the Lake Chad basin, Africa. *Scientific Reports*, 9(1), 1–18. <https://doi.org/10.1038/s41598-019-42811-9>
- Mallya, G., Mishra, V., Niyogi, D., Tripathi, S., & Govindaraju, R. S. (2016). Trends and variability of droughts over the Indian monsoon region. *Weather and Climate Extremes*, 12, 43–68. <https://doi.org/10.1016/j.wace.2016.01.002>
- McKee, T. B., Doesken, N. J., & Kleist, J. (1993). The relationship of drought frequency and duration to time scales. *Proceedings of the 8th Conference on Applied Climatology*, 17, 179–184. <https://climate.colostate.edu/pdfs/relationshipofdroughtfrequency.pdf>. Accessed 13 Mar 2023
- Mishra, A. K., & Desai, V. R. (2005). Spatial and temporal drought analysis in the Kansabati river basin, India. *International Journal of River Basin Management*, 3(1), 31–41. <https://doi.org/10.1080/15715124.2005.9635243>
- Mishra, N., Khare, D., Shukla, R., & Kumar, K. (2014). Trend analysis of air temperature time series by Mann Kendall test—A case study of upper Ganga canal command (1901–2002). *British Journal of Applied Science & Technology*, 4, 4066–4082. <https://doi.org/10.9734/BJAST/2014/8650>
- Mohammadrezaei, M., Soltani, S., & Modarres, R. (2020). Evaluating the effect of ocean-atmospheric indices on drought in Iran. *Theoretical and Applied Climatology*, 140(1), 219–230. <https://doi.org/10.1007/s00704-019-03058-6>
- Mohammed, K., Saiful Islam, A. K. M., Tarekul Islam, G. M., Alfieri, L., Bala, S. K., & Uddin Khan, Md. J. (2017). Impact of high-end climate change on floods and low flows of the Brahmaputra River. *Journal of Hydrologic Engineering*, 22(10), 04017041. [https://doi.org/10.1061/\(asce\)he.1943-5584.0001567](https://doi.org/10.1061/(asce)he.1943-5584.0001567)
- Mondal, A., & Lakshmi, V. (2021). Estimation of total water storage changes in India. *International Journal of Digital Earth*, 14(10), 1294–1315. <https://doi.org/10.1080/17538947.2021.1914759>
- Munagapati, H., & Tiwar, V. M. (2021). Spatio-temporal patterns of mass changes in himalayan glaciated region from EOF analyses of GRACE Data. *Remote Sensing*, 13(2). <https://doi.org/10.3390/rs13020265>
- Narasimha, R., & Bhattacharyya, S. (2010). A wavelet cross-spectral analysis of solar–ENSO–rainfall connections in the Indian monsoons. *Applied and Computational Harmonic Analysis*, 28, 285–295. <https://doi.org/10.1016/j.acha.2010.02.005>
- Nath, R., Nath, D., Li, Q., Chen, W., & Cui, X. (2017). Impact of drought on agriculture in the Indo-Gangetic Plain, India. *Advances in Atmospheric Sciences*, 34(3), 335–346. <https://doi.org/10.1007/s00376-016-6102-2>
- NCAR. (2023). *Climate Data Guide*. Climate data guide. <https://climatedataguide.ucar.edu/>. Accessed 28 Aug 2023
- Niranjan Kumar, K., Rajeevan, M., Pai, D. S., Srivastava, A. K., & Preethi, B. (2013). On the observed variability of monsoon droughts over India. *Weather and Climate Extremes*, 1, 42–50. <https://doi.org/10.1016/j.wace.2013.07.006>
- Panda, A., & Sahu, N. (2019). Trend analysis of seasonal rainfall and temperature pattern in Kalahandi, Bolangir and Koraput districts of Odisha, India. *Atmospheric Science Letters*, 20(10), e932. <https://doi.org/10.1002/asl.932>
- Pandey, A., Kaushik, K., & Parida, B. (2022). Google earth engine for large-scale flood mapping using SAR data and impact assessment on agriculture and population of Ganga-Brahmaputra basin. *Sustainability*, 14, 4210. <https://doi.org/10.3390/su14074210>
- Parajuli, B., Zhang, X., Deuja, S., & Liu, Y. (2021). Regional and seasonal precipitation and drought trends in Ganga-Brahmaputra basin. *Water*, 13(16), 16. <https://doi.org/10.3390/w13162218>
- Patel, A., Goswami, A., Dharpure, J. K., & Thamban, M. (2021). Rainfall variability over the Indus, Ganga, and Brahmaputra river basins: A spatio-temporal

- characterisation. *Quaternary International*, 575–576, 280–294. <https://doi.org/10.1016/j.quaint.2020.06.010>
- Paul, G. C., Saha, S., & Hembram, T. K. (2019). Application of the GIS-based probabilistic models for mapping the flood susceptibility in Bansloi Sub-basin of Ganga-Bhagirathi river and their comparison. *Remote Sensing in Earth Systems Sciences*, 2(2), 120–146. <https://doi.org/10.1007/s41976-019-00018-6>
- Pervez, M. S., & Henebry, G. M. (2015). Spatial and seasonal responses of precipitation in the Ganges and Brahmaputra river basins to ENSO and Indian Ocean dipole modes: Implications for flooding and drought. *Natural Hazards and Earth System Sciences*, 15(1), 147–162. <https://doi.org/10.5194/nhess-15-147-2015>
- Rasul, G. (2015). Water for growth and development in the Ganges, Brahmaputra, and Meghna basins: An economic perspective. *International Journal of River Basin Management*, 13(3), 387–400. <https://doi.org/10.1080/15715124.2015.1012518>
- Sajjad, H., Saha, T. K., Rahaman, M. H., Masroor, M., Sharma, Y., & Pal, S. (2023). Analyzing trend and forecast of rainfall and temperature in Valmiki Tiger Reserve, India, using non-parametric test and random forest machine learning algorithm. *Acta Geophysica*, 71(1), 531–552. <https://doi.org/10.1007/s11600-022-00978-2>
- Salas, J. D. (1993). Analysis and modelling of hydrological time series. *Handbook of hydrology* (p. 19). <https://cir.nii.ac.jp/crid/1573668924863168256>. Accessed 26 Dec 2023
- Samal, N. R., Roy, P. K., Majumadar, M., Bhattacharya, S., & Biswasroy, M. (2014). Six years major historical urban floods in West Bengal State in India: Comparative analysis using neuro-genetic model. *American Journal of Water Resources*, 2(2), 41–53. <https://doi.org/10.12691/ajwr-2-2-3>
- Seiler, R. A., Hayes, M., & Bressan, L. (2002). Using the Standardized Precipitation Index for flood risk monitoring. *International Journal of Climatology*, 22(11), 1365–1376. <https://doi.org/10.1002/joc.799>
- Shi, X., Qin, T., Nie, H., Weng, B., & He, S. (2019). Changes in major global river discharges directed into the ocean. *International Journal of Environmental Research and Public Health*, 16(8). <https://doi.org/10.3390/ijerph16081469>
- Singh, R. M., & Shukla, P. (2020). Drought characterization using drought indices and El Niño effects. *National Academy Science Letters*, 43(4), 339–342. <https://doi.org/10.1007/s40009-019-00870-6>
- Singh, S., Pandey, A., & Nathawat, M. (2011). Rainfall variability and spatio temporal dynamics of flood inundation during the 2008 Kosi flood in Bihar State, India. *Asian Journal of Earth Sciences*, 4, 9–19. <https://doi.org/10.3923/ajes.2011.9.19>
- Surmaini, E., Hadi, T. W., Subagyono, K., & Puspito, N. T. (2015). Early detection of drought impact on rice paddies in Indonesia by means of Niño 3.4 index. *Theoretical and Applied Climatology*, 121(3), 669–684. <https://doi.org/10.1007/s00704-014-1258-0>
- Trenberth, K. E., & Hoar, T. J. (1997). El Niño and climate change. *Geophysical Research Letters*, 24(23), 3057–3060. <https://doi.org/10.1029/97GL03092>
- Tripathi, G., Pandey, A. C., & Parida, B. R. (2022). Flood hazard and risk zonation in North Bihar using satellite-derived historical flood events and socio-economic data. *Sustainability*, 14(3), 3. <https://doi.org/10.3390/su14031472>
- Tripathi, G., Pandey, A. C., Parida, B. R., & Kumar, A. (2020). Flood inundation mapping and impact assessment using multi-temporal optical and SAR satellite data: A case study of 2017 flood in Darbhanga District, Bihar, India. *Water Resources Management*, 34(6), 1871–1892. <https://doi.org/10.1007/s11269-020-02534-3>
- Tsakiris, G., Tigkas, D., Vangelis, H., & Pangalou, D. (2007). Regional drought identification and assessment. Case study in Crete. In G. Rossi, T. Vega, & B. Bonaccorso (Eds.), *Methods and tools for drought analysis and management* (pp. 169–191). Springer Netherlands. [https://doi.org/10.1007/978-1-4020-5924-7\\_9](https://doi.org/10.1007/978-1-4020-5924-7_9)
- Uhe, P. F., Mitchell, D. M., Bates, P. D., Sampson, C. C., Smith, A. M., & Islam, A. S. (2019). Enhanced flood risk with 1.5 °C global warming in the Ganges-Brahmaputra-Meghna basin. *Environmental Research Letters*, 14(7). <https://doi.org/10.1088/1748-9326/ab10ee>
- UNFCCC. (2015, December 30). *Report of the conference of the parties on its twenty-first session. Part two: Action taken by the conference of the parties at its twenty-first session.* Conference of the parties, Paris. <https://unfccc.int/resource/docs/2015/cop21/eng/10a01.pdf>. Accessed 15 Mar 2023
- Webster, P. J., Magaña, V. O., Palmer, T. N., Shukla, J., Tomas, R. A., Yanai, M., & Yasunari, T. (1998). Monsoons: Processes, predictability, and the prospects for prediction. *Journal of Geophysical Research: Oceans*, 103(C7), 14451–14510. <https://doi.org/10.1029/97JC02719>
- Whitehead, P. G., Jin, L., Macadam, I., Janes, T., Sarkar, S., Rodda, H. J. E., Sinha, R., & Nicholls, R. J. (2018). Modelling impacts of climate change and socio-economic change on the Ganga, Brahmaputra, Meghna, Hooghly and Mahanadi river systems in India and Bangladesh. *Science of the Total Environment*, 636, 1362–1372. <https://doi.org/10.1016/j.scitotenv.2018.04.362>
- World Meteorological Organization (WMO), Svoboda, M., Hayes, M., & Wood, D. (2012). *Standardized Precipitation Index User Guide*. [https://library.wmo.int/doc\\_num.php?explnum\\_id=7768](https://library.wmo.int/doc_num.php?explnum_id=7768). Accessed 12 Apr 2023
- Yadav, A., Das, S., Bakar, K. S., & Chakraborti, A. (2023). Understanding the complex dynamics of climate change in south-west Australia using machine learning. *Physica a: Statistical Mechanics and Its Applications*, 627, 129139. <https://doi.org/10.1016/j.physa.2023.129139>
- Yvonne, M., Ouma, G., Olago, D., & Opondo, M. (2020). Trends in climate variables (temperature and rainfall) and local perceptions of climate change In Lamu, Kenya. *Geography, Environment, Sustainability*, 13(3), 3. <https://doi.org/10.24057/2071-9388-2020-24>

**Publisher's Note** Springer Nature remains neutral with regard to jurisdictional claims in published maps and institutional affiliations.

Springer Nature or its licensor (e.g. a society or other partner) holds exclusive rights to this article under a publishing agreement with the author(s) or other rightsholder(s); author self-archiving of the accepted manuscript version of this article is solely governed by the terms of such publishing agreement and applicable law.